J. At. Mol. Sci.
doi: 10.4208/jams.012111.022311a

Vol. **2**, No. 3, pp. 212-224
August 2011

Electronic structure, electric moments and vibrational analysis of 3-(2-methoxyphenoxy) propane-1,2-diol by *ab initio* and density functional theory

Leena Sinha, Amarendra Kumar, Vijay Narayan, Rajesh K. Srivastava, and Onkar Prasad*

Physics Department, University of Lucknow, Lucknow 226007, India

Received 21 January 2011; Accepted (in revised version) 23 February 2011
Published Online 28 March 2011

Abstract. The molecular properties and harmonic wavenumbers of 3-(2-methoxyphenoxy) propane-1,2-diol have been calculated using *ab initio* and density functional theory. The polarizability and first static hyperpolarizability of the title molecule have been calculated at different basis sets. In general a good agreement between experimental and calculated normal modes has been observed. The frontier orbital and molecular electrostatic potential surface study has also been employed to understand the active sites of 3-(2-methoxyphenoxy) propane-1,2-diol.

PACS: 31.15.A, 31.15.es, 31.15.ap

Key words: Density functional theory, frontier orbital energy gap, first static hyperpolarizability

1 Introduction

With the standard quantum chemical models (i.e., without the inclusion of parity violation), there is no difference whatsoever in energetics, vibrational frequencies, polarizabilities, NMR spectra, or any other non-chiral property for a given pair, i.e., (R) and (S) forms of enantiomers [1–4]. Differences in the properties of enantiomers arise either only within chiral environments or interactions with other chiral compounds. The present investigation therefore deals with the quantum chemical study of molecular structural, energetic and vibrational data of one of the pair i.e., (R) enantiomer of 3-(2-methoxyphenoxy) propane-1,2-diol [MPPD], in gas phase, due to its biological and pharmaceutical importance. The drug MPPD, also known as guaifenesin, is an expectorant, used extensively in anti-tussive and is capable of increasing the excretion of phlegm from the respiratory tract. Bredikhin and others have carried out

*Corresponding author. *Email address:* onkarprasad1@gmail.com (O. Prasad)

 ©2011 Global-Science Press

extensive studies on the structure, solid state properties and issues related to the effective resolution procedure for MPPD [5–7].

The vibrational spectroscopic analysis is known to provide immensely invaluable molecular structure elucidation in synergy with quantum chemical calculations. In order to obtain a complete description of molecular dynamics, vibrational wavenumber calculations along with the normal mode analysis have been carried out at the DFT level employing the basis set 6-311+G(2*d*,2*p*). The optimized geometry of molecule under investigation and its molecular properties such as equilibrium energy, frontier orbital energy gap, molecular electrostatic potential energy map, dipole moment, polarizability, first static hyperpolarizability have also been used to understand the properties and active sites of the drug.

2 Experimental

2.1 Structure and Spectra

The model molecular structure of MPPD has been given in Fig. 1. The calculated IR spectra has been shown in Fig. 2 and is found to match well with IR spectral data reported by NIST Standard Reference Database 69: NIST Chemistry Web Book [8].

3 Computational Details

Quantum chemical study of the MPPD, has been performed within the framework of Hartree Fock and the density functional theory [9] with Becke's three-parameter hybrid exchange functional [10] with Lee-Yang-Parr correlation functionals (B3LYP) [11, 12] and employing 6-311 + G(2*d*,2*p*) basis set using the Gaussian 09 program package [13]. As the DFT hybrid B3LYP functional tends to overestimate the fundamental normal modes of vibration, a scaling factor of 0.9679 has been applied and a good agreement of calculated modes with experimental ones has been obtained [14,15]. The vibrational wavenumber assignments have been carried out by combining the results of the Gaussview 5 program [16], symmetry considerations and the VEDA 4 program [17]. The calculated IR spectra have been plotted using the pure Lorentzian band shape with a band width of FWHM of 10 cm^{-1} and are shown in Fig. 2.

Density functional theory has also been used to calculate the dipole moment μ, mean polarizability α and first static hyperpolarizability β based on Finite field approach. Following Buckingham's definitions [18], the total dipole moment and the mean polarizability in a Cartesian frame is defined by

$$\mu = (\mu_x + \mu_y + \mu_z)^{1/2}, \tag{1}$$

$$\langle\alpha\rangle = \frac{1}{3}(\alpha_{xx} + \alpha_{yy} + \alpha_{zz}). \tag{2}$$

The total intrinsic hyperpolarizability β_{total} and a component of the first hyperpolarizability

along the direction of the dipole moment represented by β_μ [19,20] are defined as

$$\beta_{\text{total}} = (\beta_x^2 + \beta_y^2 + \beta_z^2)^{1/2}, \tag{3}$$

$$\beta_\mu = \frac{3}{5}(\beta_x\mu_x + \beta_y\mu_y + \beta_z\mu_z)^{1/2}, \tag{4}$$

where

$$\beta_x = (\beta_{xxx} + \beta_{xyy} + \beta_{xzz}), \quad \beta_y = (\beta_{yyy} + \beta_{yxx} + \beta_{yzz}), \quad \text{and} \quad \beta_z = (\beta_{zzz} + \beta_{zxx} + \beta_{zyy}).$$

4 Results and discussion

4.1 Molecular geometry optimization and energies

There are many possible conformations for MPPD, the conformers with lowest value of ground state energy (without any significant difference in energetics) being the (R) and (S) enan-

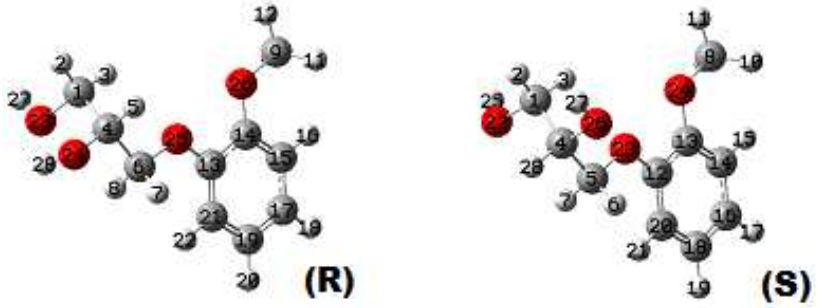

Figure 1: Optimized structure of R and S enantiomers of 3-(2-methoxyphenoxy) propane-1,2-diol.

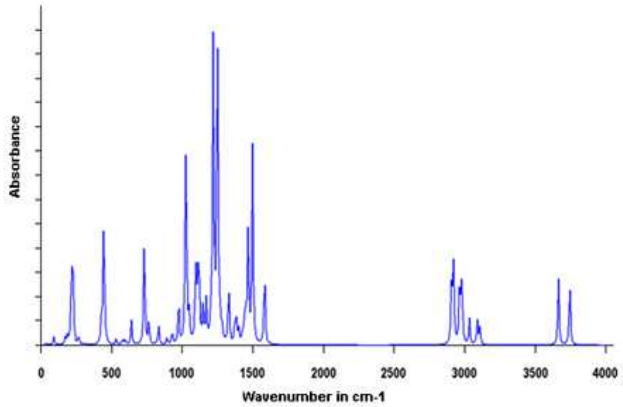

Figure 2: Theoretical IR spectra of 3-(2-methoxyphenoxy) propane-1,2-diol.

tiomers. The enantiomer couple (R) and (S) are shown in Fig. 1. The (R) enantiomer having slightly lower energy as compared to (S) [refer to Table 1], was further optimized for the calculation of its molecular properties using DFT at the B3LYP level, starting with the 6-311G(d) basis set, the polarization and the diffused functions were incorporated in steps. The X-ray diffraction data of the MPPD was obtained from Cambridge Crystallographic Data Center (CCDC 693625). The initial coordinates of the title molecule thus obtained have been used as the starting point to optimize the structure. The optimized geometry of molecule (Fig. 1) under study is confirmed to be located at the local true minima on potential energy surface, as the calculated vibrational spectra contains no imaginary wavenumber. The crystallographic data of MPPD shows that the three dimensional network of molecule is linked through hydrogen bonds [6]. The whole molecule is nearly planer except for C1 atom and the groups attached to it. The optimized structural parameters (bond lengths, bond angles, dihedral angles) of MPPD have been compared with those in X-Ray crystal structure data [6] as shown in Table 2. There are two dihedral angles in MPPD molecule involving C1 and C4 carbon atoms to which hydroxyl groups are attached, where there is a significant difference between the experimentally measured [6] and calculated values (Table 2) which has been explained briefly. The geometric differences between the optimized molecule and the molecule in solid state are due to the fact that the molecular conformation in the gas phase is different from that in the solid state, where inter molecular interactions play an important role in stabilizing the crystal structure. The deviation in the dihedral angles seem to be justified in the present case as the hydroxyl groups are involved in inter-molecular hydrogen bonding. The intra molecular hydrogen bonding between O23-H28 atoms in calculated theoretically (2.233 Å) also agrees well with the hydrogen bonding involved in the crystal packing data reported by Bredikhin *et al.* [6]. The ester (C–O) bond lengths lie in the range (1.362–1.426 Å)/(1.360–1.424 Å) is found to be close to the standard ester C–O bond lengths [21, 22]. The benzene endocyclic C–C–C angles are found to lie in the range 119.30°– 120.60°. These calculated bond length, bond angles are in full agreement with those standard bond lengths and bond angles.

According to the calculations all the oxygen atoms in the title molecule carry a net negative charge. The charge on oxygen atom O(23) and O(25) being the highest and lowest respectively.

Table 1: Ground state optimized parameters at DFT/B3LYP level of theory for 3-(2-methoxyphenoxy) propane-1,2-diol.

Parameters	6-311+G(2d,2p)	
	HF	B3LYP
Ground state energy (in Hartree)	-686.45758 (R) -686.45710 (S)	-690.57982 (R) -690.57564 (S)
Frontier orbital energy gap (in eV)	6.38352	5.48935
Diploe moment (in Debye)	2.79	2.78

Table 2: Comparison of optimized interatomic distances (Bond lengths in Å), bond angles and dihedral angles in degrees of 3-(2-methoxyphenoxy) propane-1,2-diol (R) at B3LYP/ 6-311+G(2d,2p) level with X-Ray data.

Interatomic distance	B3LYP Bond length	X-Ray data	Bond angles	B3LYP Bond angles	X-Ray data
C1–H2	1.093	0.970	C9–O26–C14	118.0	116.6
C1–H3	1.091	0.971	O26–C14–C13	115.6	115.6
C4–H5	1.091	0.980	O14–C13–O25	115.7	115.6
C6–H8	1.093	0.969	C13–O25–C6	118.7	116.8
C6–H7	1.092	0.969	O25–C6–C4	107.4	107.4
C9–H10	1.093	0.960	C6–C4–C1	113.0	113.5
C9–H11	1.093	0.960	C6–C4–O24	109.2	105.4
C9–H12	1.086	0.960	C4–C1–O23	106.9	112.0
C4–O24	1.423	1.433	C21–C13–O25	124.9	124.7
C6–O25	1.424	1.428	C1–O23–H27	109.4	107.4
C13–O25	1.362	1.368	C4–C1–H3	109.8	109.2
C14–O26	1.363	1.370	C4–C1–H2	109.0	109.2
C9–O26	1.412	1.422	O25–C6–H7	110.8	110.3
O24–H28	0.965	0.912	O25–C6–H8	110.5	110.2
O23–H27	0.959	0.867			

Dihedral angle	B3LYP value	X-ray data
O24–C4–C6–O25	172.12	177.23
C4–C6–O25–C13	179.8	177.7
O23–C1–C4–C6	67.5	51.2
C1–C4–C6–O25	63.9	54.1
C6–O25–C13–C14	178.6	174.9
O25–C13–C14–O26	0.2	0.2
C13–C14–O26–C9	-179.21	-168.7

4.2 Electronic properties

The highest occupied molecular orbital (HOMO) is the orbital that primarily acts as an electron donor and the lowest unoccupied molecular orbital (LUMO) is the orbital that largely acts as the electron acceptor. The frontier orbital energy gap helps characterize the chemical reactivity and kinetic stability of the molecule. The 3D plots of the frontier orbitals HOMO, LUMO and the Molecular electrostatic potential map (MESP) figures for MPPD are shown in Figs. 3 and 4 respectively. It can be seen from Fig. 3, that the HOMO is spread heavily over the phenyl ring region. The HOMO also shows appreciable čk bonding character. In contrast the LUMO display Rydberg character at the alcoholic end and are located outside the molecule and oriented perpendicular to the molecular plane. Consequently the HOMO to LUMO transition reflects the transfer of electron cloud mainly from phenyl ring to Rydberg type excited state. The electron thus transferred to the Rydberg state is very weakly bound to the rest

of the molecule. This electron spends most of its time a long way from the molecule. The basis set 6-311G+(2d,2p) which includes asymptotically correct functions with slower radial decay to represent a more diffuse electron distribution in addition to additional polarization functions, has been suitably chosen to describe the LUMO orbitals adequately. The frontier orbital energy gap in case of MPPD is found to be 5.48934 eV.

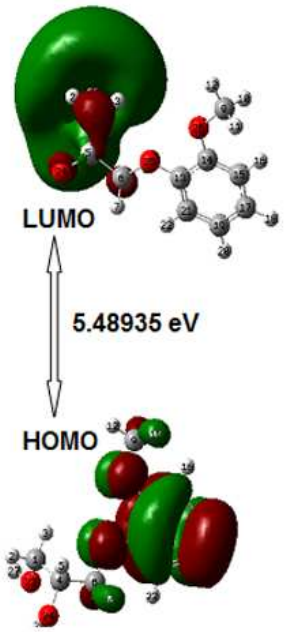

Figure 3: HOMO-LUMO plot of 3-(2-methoxyphenoxy) propane-1,2-diol.

The value of the electrostatic potential (the energy of interaction of a positive test point charge with the nuclei and electrons of a molecule) mapped onto an electron iso-density surface may be employed to distinguish regions on the surface which are electron rich (subject to electrophilic attack) from those which are electron poor (subject to nucleophilic attack). When the two molecules are structurally very similar, molecular electrostatic potential surfaces make clear that this similarity does not carry over into their electrophilic/nucleophilic reactivities. The resulting surface simultaneously displays molecular size, shape and electrostatic potential in terms of colour grading and is very useful tool in investigation of correlation between molecular structure and the physiochemical property relationship of molecules including biomolecules and drugs [23–30]. The variation in electrostatic potential produced by a molecule is largely responsible for the binding of a drug to its receptor binding sites, as the binding site in general is expected to have opposite areas of electrostatic potential. The MESP for the title molecule is shown in Fig. 4. The MESP map in case of the MPPD clearly suggests that the potential swings wildly between alcoholic oxygen (dark red) and alcoholic hydrogen atoms which bear most the brunt of positive charge (blue). There is only one ac-

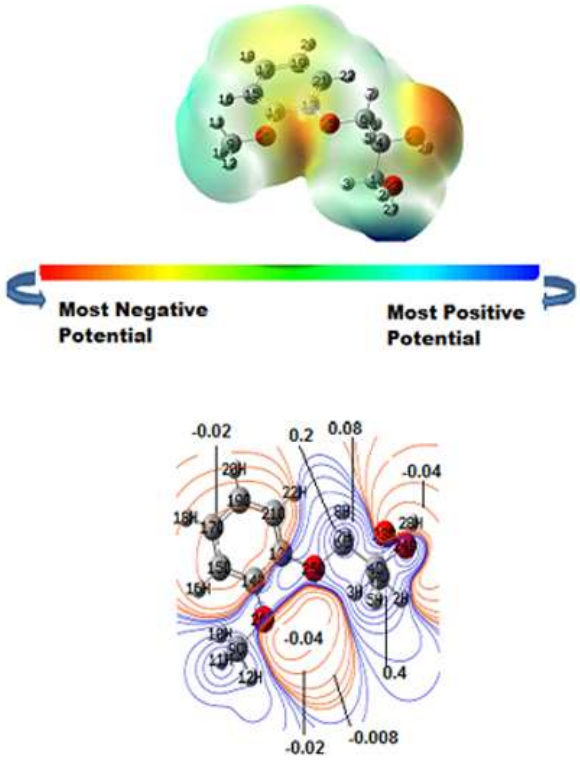

Figure 4: MESP surface and contour plots of 3-(2-methoxyphenoxy) propane-1,2-diol. Contours are drawn 1.4 Å above the molecular plane.

tive electrophilic site. The larger extent of spread of green colour which corresponds to a potential halfway between the two extremes red and blue colour suggests that most part of the molecule has almost the neutral potential. The sliced 2D MESP contour map of the title molecule has also been plotted in Fig. 4. Such a representation provides more detailed information regarding electrostatic potential distribution, by showing the values in a manifold of spatial location around the molecule. The MESP 2D contour maps for MPPD is drawn in the plane 1.4 Å above the molecular plane. These maps clearly shows that the maximum value of positive and negative potential are 0.4 a.u. and -0.04 a.u. respectively.

4.3 Electric moments

The origin of intermolecular interactions involving the van der Waal type dipole-dipole forces etc. is mainly attributed to an overall imbalance in charge from one side of a molecule to the

other side. The calculated dipole moment value is 2.78 Debye for MPPD (refer to Table 1).

The extensive and important studies on electric polarizability and hyperpolarizability, by Maroulis and others [31–35], emphasize the relative importance of electron correlation, choice of basis set and the different methods employed for the calculation of these quantities. Consequently the electric polarizability and hyperpolarizability have been calculated at different basis sets employing different level of theories to arrive at the better description of these quantities for the title molecule under investigation in absence of experimental data. The mean polarizability, components of β, total intrinsic hyperpolarizability (β_{total}) and the component of the hyperpolarizability along the direction of the dipole moment μ are presented in Table 3. The variation in polarizability and hyperpolarizability with the addition of the basis functions at HF and B3LYP is plotted in Figs. 5 and 6 respectively.

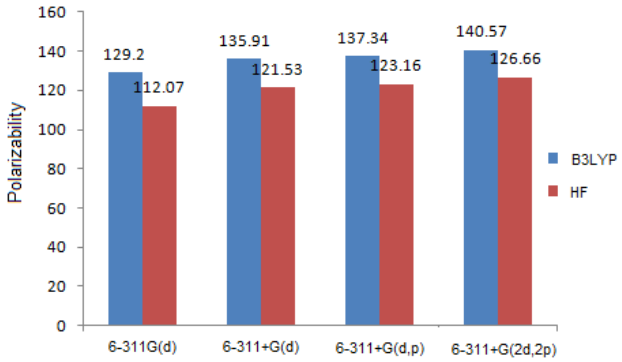

Figure 5: Basis set effects on the polarizability of 3-(2-methoxyphenoxy) propane-1,2-diol.

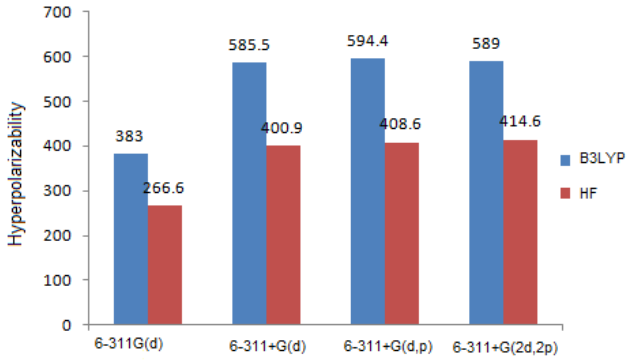

Figure 6: Basis set effects on the hyperpolarizability of 3-(2-methoxyphenoxy) propane-1,2-diol.

Table 3: Polarizability[a] data and hyperpolarizability[b] data 3-(2-methoxyphenoxy) propane-1,2-diol calculated at HF/6-311+G(2*d*,2*p*) and DFT/ B3LYP/6-311+G(2*d*,2*p*) level of theory.

Polarizability[a]	HF	B3LYP
α_{XX}	149.43	169.25
α_{YY}	137.82	153.23
α_{ZZ}	92.75	99.24
$\langle\alpha\rangle$	126.66	140.56
Hyperpolarizability[b]		
β_{XXX}	-210.5	-331.9
β_{XXY}	-40.2	-54.4
β_{XYY}	-56.0	-77.8
β_{YYY}	-138.7	-212.0
β_{XXZ}	8.4	28.5
β_{XYZ}	-5.5	2.1
β_{YYZ}	1.5	12.2
β_{XZZ}	-75.7	-82.4
β_{YZZ}	-51.4	-47.8
β_{ZZZ}	32.1	36.8
β_{total}	414.6	589.0
β_{μ}	-36.1	-131.1

[a] In atomic units. Conversion factor to the SI units- $1e^2a_0{}^2E_h{}^{-1} = 1.648\,778 \times 10^{-41}$ C^2 m^2 J^{-1}.

[b] In atomic units. Conversion factor to the SI units- $1e^3a_0{}^3E_h{}^{-2} = 3.206\,361 \times 10^{-53}$ C^3 m^3 J^{-2}.

4.4 Vibrational assignments

The optimized molecular structure belong to the C1 point group as it does not display any special symmetry. The overestimation of the vibrational wavenumbers in *ab initio* and DFT methods are corrected either by computing anharmonic correlations explicitly or by introducing a scaled field [14], even directly scaling the calculated wavenumbers with proper factor. The vibrational wavenumbers are calibrated accordingly with the scaling factor of 0.9679 for DFT at B3LYP [15]. The vibrational assignments have been done on the basis of relative intensities, line shape, the VEDA 4 program and the animation option of Gaussview 5. The experimental and scaled calculated wave numbers along with their respective dominant modes are presented in Table 4.

The calculated vibrational spectra of MPPD has been divided in two regions; a low wavenumber fingerprint region (<2000 cm^{-1}) and a high wavenumber functional group region (4000– 2000 cm^{-1}). A total of 78 (3N-6) normal modes of vibrations have been calculated for MPPD. The functional group and fingerprint regions have 14/ 64 normal modes of vibrations in MPPD.

Table 4: Theoretical and experimental* wave numbers of 3-(2-methoxyphenoxy) propane-1,2-diol.

Scaled wave no. in cm^{-1}	Exp.* IR wave no. in cm^{-1}	Assignment of dominant modes in terms of potential energy distribution (PED)
3741	3243	ν(O23–H27)(100)
3663	3074	ν(O24–H28)(100)
3107	–	ν_s ((C–H))R(92)
3101	–	ν_{as} ((C–H))R(91)
3085	–	ν_{as} ((C–H))R(94)
3069	–	ν_{as} ((C–H))R(95)
3030	3009	ν_{as} CH_3(92)
2977	–	ν (C4–H5)(63)+ ν_{as} ($C6H_2$)(36)
2971	–	ν_{as} ($C1H_2$)(99)
2961		ν_{as} ($C6H_2$)(64) + ν(C4–H5)(34)
2960	2942	ν_{as} CH_3(100)
2920	–	ν_s ($C6H_2$)(63)+ ν_s ($C1H_2$)(27)
2918		ν_s ($C1H_2$)(62) + ν_s($C6H_2$)(36)
2905	2887	ν_s CH_3(92)
1580	1594	ν(C–C)R(38) + β(C–C–C) R(22)+ β(H–C–C)R(10)
1576	–	ν(C–C)R(71)
1491	1525	β(H–C–C)R(34)+ ν(C–C)R(17)
1462	1468	sc($C6H_2$)(58) + sc($C1H_2$)(15)
1460	1455	sc($C1H_2$)(56) + sc($C6H_2$)(21)
1458	1455	CH_3 as. Deformation(78)
1445	1441	CH_3 as. Deformation(93)
1438	–	β(H–C–C)R(34)+ CH_3 umbrella bending (12) + ν(C–C)R (11)
1423	–	CH_3 umbrella bend(50) + β(H–C–C)R(14)
1395	1383	ω(C4–H5)(16)+β(H28–O24–C4)(14)+β(H27–O23–C1)(12)
1379	1376	ω($C6H_2$)(26)+ω(C4–H5)(18)+β(H28–O24–C4)(15)
1368	–	ω(C4–H5)(29)+ω($C6H_2$)(12)+ω($C1H_2$)(18)+ β(H28–O24–4)(10)
1322	1330	ω(C4–H5)(44)+ ω($C6H_2$)(12)
1319	1295	ν(C–C)R(43) + ω($C6H_2$)(16) + ω(C4–H5)(11)
1272	1267	β(H–C–C)R(54)
1256	–	ω($C1H_2$)(26)+ω(C4–H5)(20)+β(H28–O24–C4)(16)
1242	–	ω($C1H_2$)(15)+ω ($C6H_2$)(15)+ ν(O26–C14)(10)
1238	1231	ω($C1H_2$)(24)+ω($C6H_2$)(24)+ ν(C–C)R(10)
1212	1223	ν(O25–C13)(23) +ν(O26–C14)(20) + β (H–C–C)R(16)
1195	1187	ω($C6H_2$)(49)+ω($C1H_2$)(15)+β(H28–O24–C4)(10)
1162	1180	r(CH_3)(65)
1149	–	β (H–C–C)R(65) +ν(C–C)R(11)
1139	1129	β(H27–O23–C1)(44)+r($C1H_2$)(15)+β(H28–O24–C4)(13)+ ω(C4–H5) (12)
1131	–	r(CH_3)(99)
1110	1107	ν(C–C)R(32)+ β(H–C–C)R(24)
1101	–	ν(C4–C6)(26)+β(H27–O23–C1)(14)+ r($C1H_2$)(13)
1088	1088	ν(C1–C4)(20)+ ν(O24–C4)(17)+ ν(O23–C1)(14)
1042	1058	ν(C–C)R (22)+ ν(O26–C9)(13)+β (H–C–C)R(21)
1023	1044	ν(O23–C1)(17)+ ν(O24–C4)(16)+ r($C6H_2$)(15)
1022	1022	ν(O24–C4)(34)+ R Breathing(30)+ r($C6H_2$)(14)
1017	995	ν(O25–C6)(50)+R trigonal bending(24)+ ν(O26–C9)(12)
966	–	ν(O24–C4)(34)+ν(C6–C4)(12)+ν(O23–C1)(37) +r($C6H_2$)(14)
964	935	(C–H) R wag(73)
919	911	r($C1H_2$)(26) +ν(O24–C4)(18)+ ν(O23–C1)(12)
884	838	(C–H) R wag(80)
825	–	ν(C1–C4)(24)+ β(H–C–C) R(15) + r($C6H_2$) (10)
819	–	(C–H) R wag(53) + ρ(C–C–C–C) R(21)
804	–	ν(C1–C4)(34)+ β(C–C–C) R(22)
756	769	β(C–C–C) R(50)+ r(CH_3)(23)
729	744	ρ (C–C–C–C) R(64)+ (C–H) R wag(26)
723	–	(C–H) R wag(83)
633	641	β(O23–C1–C4)(28)+β(O24–C4–C1)(25)+ r($C6H_2$)(16)
588	–	β (C–C–C) R (44)+ r($C1H_2$)(11)
567	–	r(CH_3) (29) + β(O26–C14–C15) (27) + β(O25–C13–C21)(12)
557	–	ρ(C–C–C–C)R(62)+ρ(O26–C13–C15–C14)(11)+ρ(O25–C14–C21–C13)(11)
523	–	β(C–C–C)R(31)+ β(C4–C6–O25)(12)+ β(O24–C4–C6)(10)
456	–	ρ(C–C–C–C)R(23)+ρ(H–C–C–C)R(20) +ρ(O26–C13–C15–C14)(12) +ρ(O25–C14–C21–C13)(12)
436	–	β_{out}(H28–O24–C4)(55)+β(C6–C4–O24)(19)
420	–	β_{out}(H28–O24–C4)(39)+β(C6–C4–O24)(18)

*Experimental IR data as reported in NIST Chemistry Web Book:
`http://webbook.nist.gov/chemistry/form-ser.html`. Abbreviations used here have following meanings. ν: stretching; ν_s: symmetric stretching; ν_{as}: asymmetric stretching; β: in plane bending; β_{out}: out of plane bending; ρ: torsion; sc: scissoring; ω: wagging; γ: twisting; r: rocking; R: phenyl ring.

O–H vibrations

The O-H stretching vibration is very sensitive to hydrogen bonding. A free hydroxyl group or a non-hydrogen bonded hydroxyl group absorbs in the range 3700-3500 cm^{-1}. The intra-molecular hydrogen bonding present in the system reduces the hydroxyl stretching band to 3559-3200 cm^{-1} region [36]. The scaled wavenumber calculated at 3741 cm^{-1} and 3663 cm^{-1} in the case of MPPD are identified as O–H stretching with 100% contribution to P.E.D. The large variation in the calculated O–H stretching vibrational wavenumbers with the experimental ones may also be attributed due to the existence of four strong hydrogen bonding sites in 3-(2-ethoxyphenoxy) propane-1,2-diol as reported by Bredikhin *et al.* [6].

CH_2 vibrations

MPPD has two methylene groups, at the C1 and C6 according to the numbering scheme (Fig. 1). The asymmetric stretching of CH_2 group is calculated in the range 2977–2961 cm^{-1} whereas symmetric stretching lies in the range 2920–2918 cm^{-1}. The twisting and rocking modes of methylene group are calculated to be mixed modes and start appearing around 1260 cm^{-1}. The major methylene scissoring modes at 1462 and 1460 cm^{-1} are matched well with experimental wavenumbers. The methylene wagging modes are calculated in the range 1380–1320 cm^{-1} for the MPPD.

CH_3 group modes

The methyl group shows several characteristic fundamental vibrations corresponding to asymmetric and symmetric stretches, bending, rocking, and torsion modes. The CH_3 asymmetric stretching vibrations are generally observed in the region of 2980–2940 cm^{-1}, while the symmetric stretching vibrations usually appear between 2890 and 2850 cm^{-1}. The wavenumbers for asymmetric CH_3 stretching modes are calculated at 3030 cm^{-1} and 2960 cm^{-1} while the wavenumber of symmetric stretching vibrations calculated at 2905 cm^{-1} and are assigned to well to the experimental values. Methyl asymmetric deformation modes appear as dominant mode at 1458, 1445 cm^{-1} (with more than 65% contribution to the total P.E.D.) are assigned to 1455 cm^{-1} and 1441 cm^{-1} peak in the IR spectra. The methyl umbrella bending modes calculated for the present case are in the wavenumber range of 1440-1420 cm^{-1}. These bending modes are in general mixed with ring (H–C–C) bending modes (Table 6). The dominant methyl rocking modes are calculated to be at 1162 and 1131 cm^{-1}.

C–C and C–H vibrations

C–C stretching wavenumbers are observed as mixed modes in the range 1100 cm^{-1} to 800 cm^{-1} and agree well with the general appearance of C–H and C–C stretching modes. C–C stretches are calculated to be 1101, 1088, 966, 825 and 804 cm^{-1}. The C–H stretching vibration [ν(C4–H5)] is calculated at 2977 cm^{-1}.

Ring vibrations

The phenyl ring spectral region predominantly involves the C–H, C–C and C=C stretching, and C–C–C as well as H–C–C-bending vibrations. The bands due to the ring C–H-stretching

vibrations were observed as a group of partially overlapping absorptions in the region 3110-3069 cm^{-1} with more than 90% potential energy contribution. Vibrations involving C–H in-plane bending are found in the region 1600-825 cm^{-1}. The computed wavenumbers at 1017 cm^{-1} are identified as the trigonal ring bending and 1022 cm^{-1} as ring breathing modes respectively. The dominant phenyl ring wagging modes are calculated 964, 884 and 723 cm^{-1}. A good agreement between the calculated and experimentally observed wavenumbers has allowed establishing a detailed and precise assignment of normal mode wavenumbers in the entire spectral region.

5 Conclusions

The present study on 3-(2-methoxyphenoxy) propane-1,2-diol, comprised of equilibrium geometries optimization and the calculation of molecular ground state properties at DFT/6-311+G(2d,2p) level. The electric polarizability and hyperpolarizability have also been calculated at different basis sets employing different level of theories to arrive at the better portrayal of these quantities for the title molecule under investigation. In general, a good agreement between experimental and calculated normal modes has been observed. The structure activity relationship based on the study of frontier orbital gap, dipole moment data, electric polarizability and first static hyperpolarizability along with the molecular electrostatic potential map of the 3-(2-methoxyphenoxy) propane-1,2-diol, has been used to understand the active sites of the molecule under study.

Acknowledgments. Research support is gratefully acknowledged from Authors (OP and LS) and to UGC, India for the financial support and to Prof Jamroz for providing his VEDA 4 software. We would also like to thank Prof. Jenny Field for providing the crystal data of (R) enantiomer of MPPD.

References

[1] G. Boon, C. V. Alsenoy, F. D. Proft, *et al.*, J. Phys. Chem. A 110 (15) (2006) 5114.
[2] S. Janssens, C. V. Alsenoy, and P. Geerlings, J. Phys. Chem. A 111 (16) (2007) 3143.
[3] K. Le Barbu, A. Zehnacker, F. Lahmani, *et al.*, Chirality 13 (10) (2001) 715.
[4] H. F. Skinner, Forensic Science International 48 (1990) 128.
[5] Z. A. Bredikhina, V. G. Novikova, D. V. Zakharychev, and A. A. Bredikhin, Tetrahedron: Asymmetry 17 (2006) 3015.
[6] A. A. Bredikhin, A. T. Gubaidullin, Z. A. Bredikhina, *et al.*, J. Mol. Struct. 920 (2009) 377.
[7] A. A. Bredikhin, Z. A. Bredikhina, D. V. Zakharychev, and A. V. Pashagin, Tetrahedron: Asymmetry 18 (2007) 1239.
[8] `http://webbook.nist.gov/chemistry/form-ser.html`.
[9] W. Kohn and L. J. Sham, Phys. Rev. 140 (1965) A1133.
[10] A. D. Becke, J. Chem. Phys. 98 (1993) 5648.
[11] C. Lee, W. Yang, and R. G. Parr, Phys. Rev. B 37 (1988) 785.
[12] B. Miehlich, A. Savin, H. Stoll, and H. Preuss, Chem. Phys. Lett. 157 (1989) 200.

[13] M. J. Frisch, G. W. Trucks, H. B. Schlegel, *et al.*, Gaussian 09, Rev. A. 1 (Gaussian, Inc., Wallingford CT, 2009).
[14] A. P. Scott, L. Random, J. Phys. Chem. 100 (1996) 16502.
[15] P. Pulay, G. Fogarasi, G. Pongor, *et al.*, J. Am. Chem. Soc. 105 (1983) 7037.
[16] Æ. Frisch, H. P. Hratchian, R. D. Dennington II, *et al.*, GaussView, Version 5.0 (Gaussian, Inc., Wallingford CT, 2009).
[17] M. H. Jamroz, Vibrational Energy Distribution Analysis: VEDA 4 Program (Warsaw, Poland, 2004).
[18] A. D. Buckingham, Adv. Chem. Phys. 12 (1967) 107.
[19] D. R. Kanis, M. A. Ratner, and T. J. Marks, Chem. Rev. 94 (1994) 195.
[20] G. Maroulis, J. Chem. Phys. 113 (2000) 1813.
[21] M. Ladd, Introduction to Physical Chemistry, third ed.(Cambridge University Press, Cambridge, 1998).
[22] F. H. Allen, O. Kennard, D. G.Watson, *et al.*, J. Chem. Soc., Perkin Trans. II (1987) S1-S19.
[23] I. Fleming, Frontier Orbitals and Organic Chemical Reactions (John Wiley and Sons, New York, 1976).
[24] J. S. Murray and K. Sen, Molecular Electrostatic Potentials, Concepts and Applications (Elsevier, Amsterdam, 1996).
[25] I. Alkorta and J. J. Perez, Int. J. Quant. Chem. 57 (1996) 123.
[26] E. Scrocco and J. Tomasi, in: Advances in Quantum Chemistry, ed. P. Lowdin (Academic Press, New York, 1978).
[27] F. J. Luque, M. Orozco, P. K. Bhadane, and S. R. Gadre, J. Phys. Chem. 97 (1993) 9380.
[28] J. Sponer and P. Hobza, Int. J. Quant. Chem. 57 (1996) 959.
[29] R. K. Pathak and S. R. Gadre, J. Chem. Phys. 93 (1990) 1770.
[30] S. R. Gadre and I. H. Shrivastava, J. Chem. Phys. 94 (1991) 4384.
[31] G. Maroulis, D. Begue, and C. Pouchan, J. Chem. Phys. 119 (2003) 794.
[32] G. Maroulis, P. Karamanis, and C. Pouchan, J. Chem. Phys. 126 (2007) 154316.
[33] G. Maroulis, J. Chem. Phys. 129 (2008) 044314.
[34] J. M. Stout and C. E. Dykstra, J. Am. Chem. Soc. 117 (1995) 5127.
[35] M. A. Spackman, J. Chem. Phys. 93 (1989) 7594.
[36] M. Jag, Organic Spectroscopy - Principles and Applications, 2nd ed. (Narosa Publishing House, New Delhi, 2001).